Supplementary Material for: Photostriction-Driven Phase Transition in Layered Chiral $NbOX_2$ Crystals: Electric-Field-Controlled Enantiomer Selectivity

Jorge Cardenas-Gamboa,[1,*] Martin Gutierrez-Amigo,[2] Aritz Leonardo,[3,4] Gregory A. Fiete,[5,6,7,8] Juan L. Mañes,[9,4] Jeroen van den Brink,[1,10] Claudia Felser,[11] and Maia G. Vergniory[3,12,13,†]

[1] *Leibniz Institute for Solid State and Materials Research, IFW Dresden, Helmholtzstraße 20, 01069 Dresden, Germany*
[2] *Department of Applied Physics, Aalto University School of Science, FI-00076 Aalto, Finland*
[3] *Donostia International Physics Center, Donostia-San Sebastian 20018 Gipuzkoa, Spain*
[4] *EHU Quantum Center, University of the Basque Country UPV/EHU, 48940 Leioa, Spain*
[5] *Northeastern University, Boston, Massachusetts 02115, USA*
[6] *Quantum Materials and Sensing Institute, Northeastern University, Burlington, Massachusetts 01803, USA*
[7] *Department of Physics, Massachusetts Institute of Technology, Cambridge, MA 02139, USA*
[8] *Department of Physics, Harvard University, Cambridge, MA 02138, USA*
[9] *Physics Department, University of the Basque Country (UPV/EHU), Bilbao, Spain*
[10] *Würzburg-Dresden Cluster of Excellence Ct.qmat, Technische Universitat Dresden, 01062, Dresden, Germany*
[11] *Max Planck Institute for Chemical Physics of Solids, 01187 Dresden, Germany*
[12] *Département de physique et Institut quantique, Université de Sherbrooke, Sherbrooke J1K 2R1 QC, Canada*
[13] *Regroupement Québécois sur les Matériaux de Pointe (RQMP), Quebec H3T 3J7, Canada*

(Dated: January 7, 2026)

* jicg1@ifw-dresden.de
† maia.vergniory@usherbrooke.ca

I. COMPARISON OF VAN DER WAALS TREATMENTS

Given the layered nature of $NbOX_2$ (Fig. 1(a)), we tested several approaches for incorporating van der Waals (vdW) interactions in structural relaxations. Calculations were performed without spin–orbit coupling (SOC), starting from the experimental lattice parameters reported in Ref. [1]. We benchmarked three schemes: (i) Grimme's empirical DFT-D2 correction [2], (ii) Grimme's DFT-D3 correction [3], and (iii) a reference case without vdW corrections. The resulting relaxed lattice parameters were compared against experimental data (see Fig. 1). Among the tested schemes, DFT-D2 gave the best agreement, particularly along the interlayer axis, confirming its suitability for describing vdW interactions in this family. Therefore, all subsequent calculations employed the DFT-D2 correction.

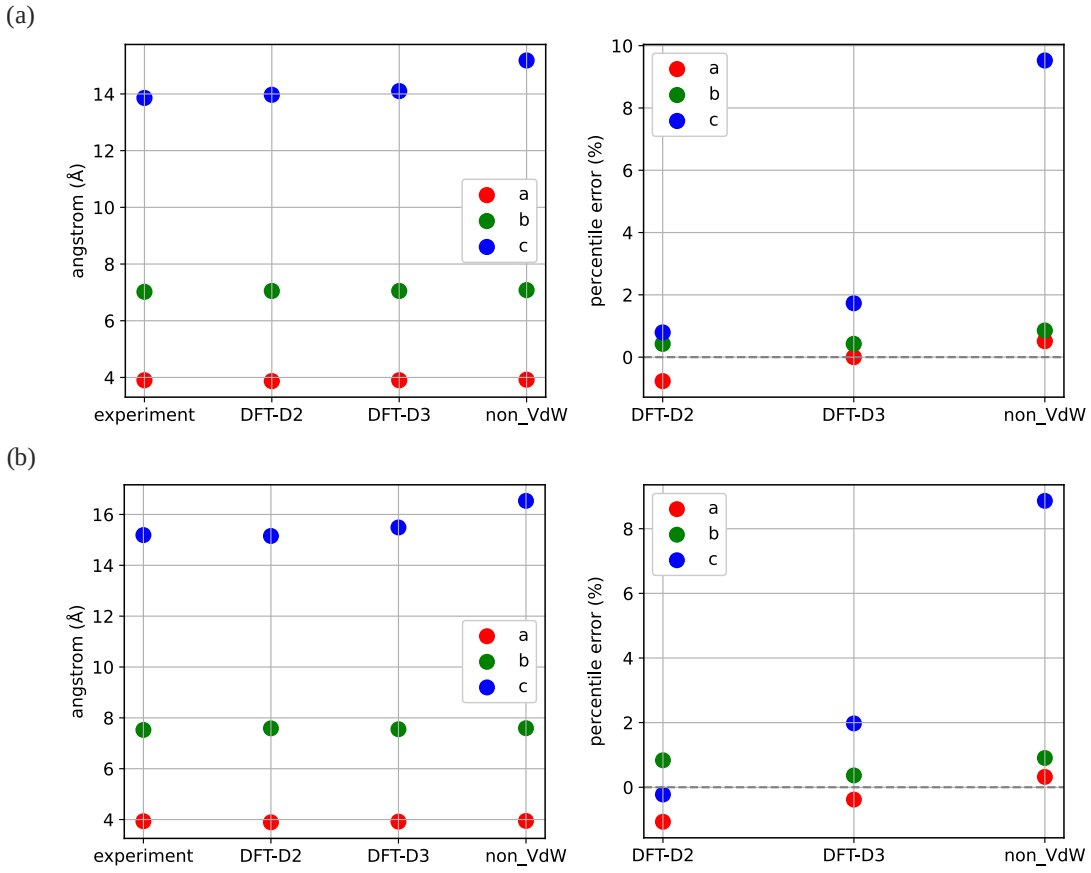

FIG. 1. Comparison of van der Waals (vdW) treatments for (a, left) $NbOBr_2$ and (b, left) $NbOI_2$. Experimental lattice parameters are taken from Ref. [1]. Panels (a, right) and (b, right) show the relative percentage error of each vdW scheme with respect to experiment.

II. BAND STRUCTURES AND PHONON SPECTRA AT DIFFERENT PHOTOCARRIER CONCENTRATIONS

For the structures analyzed in Fig. 1(c–e), we report the corresponding electronic band structures and phonon spectra (calculated under dark conditions) at two representative photocarrier concentrations: (i) $n_e = 0$, corresponding to the ground state, and (ii) $n_e = n_c$, where n_c denotes the critical carrier density required to drive the chiral-to-achiral ($C2/m$) phase transition (see dashed purple line in Fig. 2(c–e)). The results, presented in Fig. 2, show that in the achiral phase all $NbOX_2$ compounds exhibit phonon instabilities, confirming that this structure is dynamically unstable.

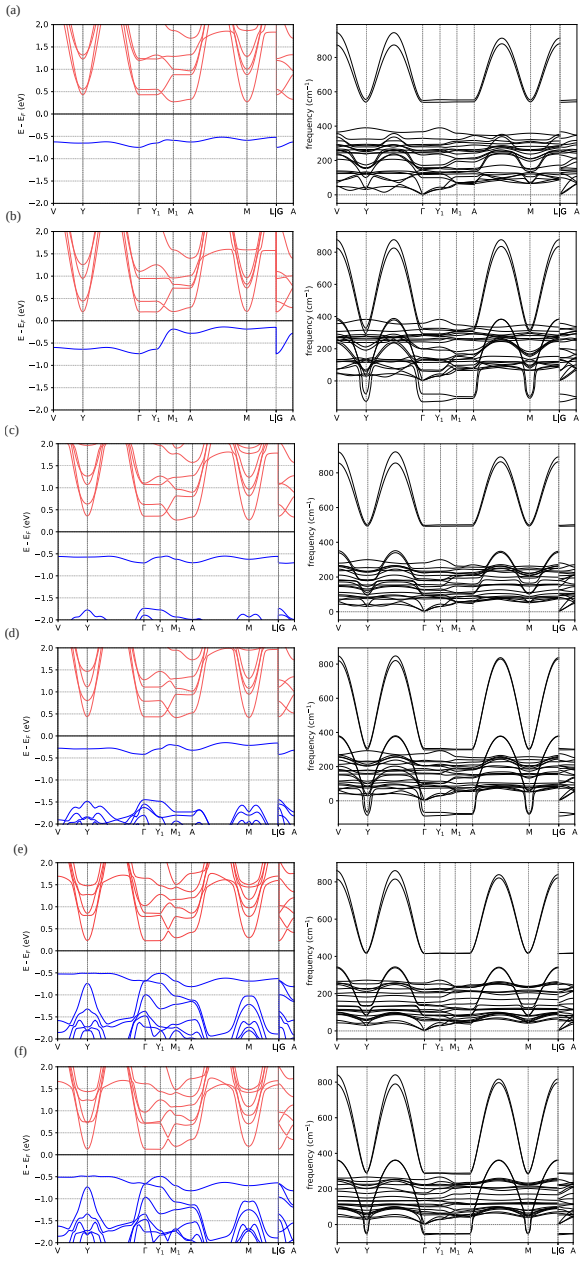

FIG. 2. Electronic band structures and phonon spectra of $NbOX_2$ at two representative photocarrier concentrations. (a,b) $NbOCl_2$ at $n_e = 0$ (ground state) and $n_e = 0.35$ e^-/f.u., respectively. (c,d) $NbOBr_2$ at $n_e = 0$ and $n_e = 0.20$ e^-/f.u. (e,f) $NbOI_2$ at $n_e = 0$ and $n_e = 0.15$ e^-/f.u. In all cases, $n_e = 0$ corresponds to the equilibrium monoclinic phase, while finite carrier concentrations illustrate the critical regimes driving the chiral-to-achiral transition.

III. PROJECTED BAND-STRUCTURE

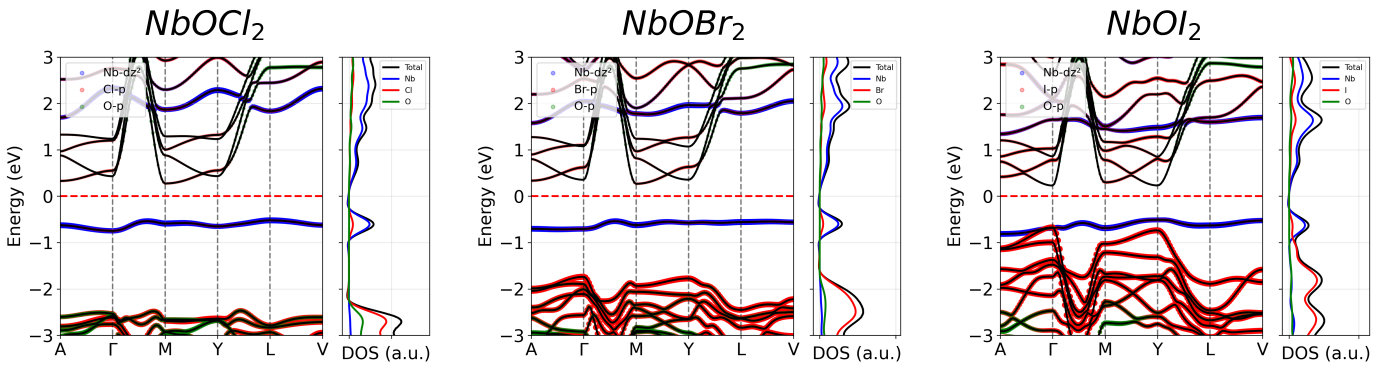

FIG. 3. Orbital-resolved band structure and density of states (DOS) of bulk $NbOX_2$ in the monoclinic ($C2$) ground state. The contribution of the Nb-d_{z^2} orbital is highlighted by blue points in the band structure.

IV. OPTICAL ABSORPTION OF BULK $NBOX_2$

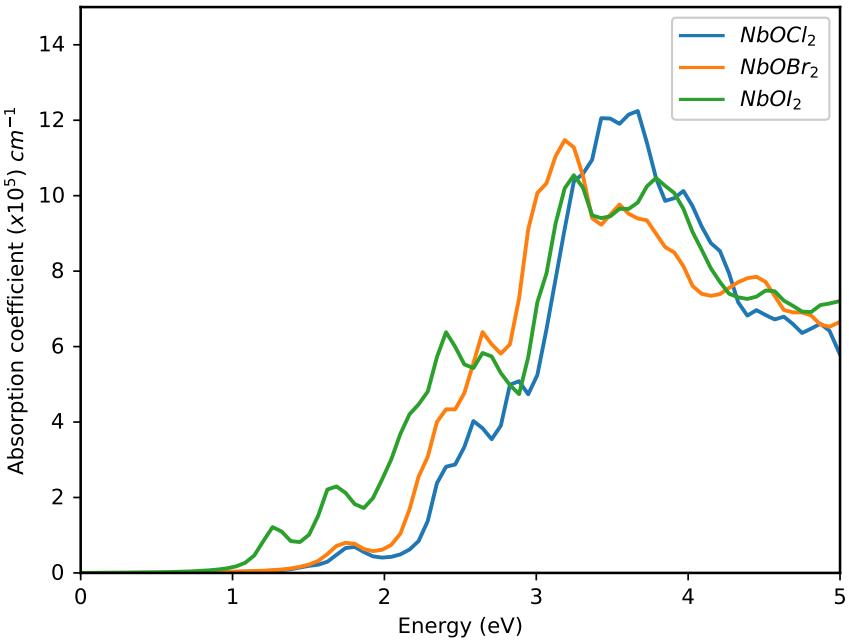

FIG. 4. Calculated optical absorption coefficient (α) of ferroelectric $NbOX_2$ bulk, obtained using the DFT-D2 functional. The spectra highlight the energy ranges relevant for photoexcitation processes and allow comparison of absorption edges across different halides. These results provide the basis for estimating the photocarrier concentrations required to drive the chiral-to-achiral transition.

V. LANDAU MODEL FOR FERROELECTRIC $NBOX_2$

The ferroelectric behavior of $NbOX_2$ can be described within the Landau free-energy expansion [4, 5]:

$$F(P) = \tfrac{1}{2}aP^2 + \tfrac{1}{4}bP^4 + \tfrac{1}{6}cP^6 - EP, \tag{1}$$

where P is the polarization, a, b, and c are expansion coefficients, and E is the applied electric field. The coefficients were obtained by fitting the Berry-phase polarization energies to Eq. 1, as shown in Fig. 2(c).

The equilibrium polarization corresponds to the minima of $F(P)$, determined by the stationary condition

$$\frac{\partial F}{\partial P} = 0, \tag{2}$$

which leads to the constitutive relation

$$E = aP + bP^3 + cP^5. \tag{3}$$

Solving Eq. 3 yields the polarization–electric field (P–E) characteristics. From these, we extracted the coercive field E_c for bulk $NbOX_2$, i.e., the minimum external field required to reverse the spontaneous polarization. The computed P–E loops and the corresponding coercive fields are presented in Fig. 5.

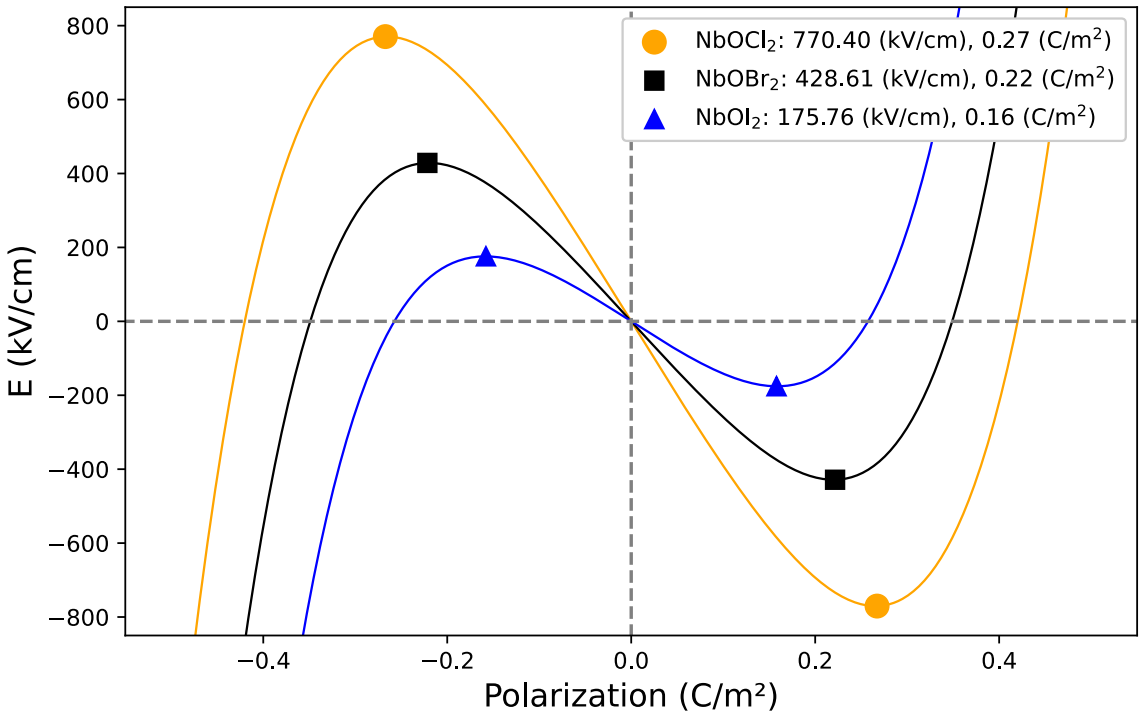

FIG. 5. Polarization–electric field (P–E) characteristics of bulk $NbOX_2$ derived from the Landau free-energy expansion. The coercive field E_c and spontaneous polarization values extracted from the fits are indicated in the legend.

[1] T. Fu, K. Bu, X. Sun, D. Wang, X. Feng, S. Guo, Z. Sun, Y. Fang, Q. Hu, Y. Ding, *et al.*, Manipulating peierls distortion in van der waals nbox2 maximizes second-harmonic generation, Journal of the American Chemical Society **145**, 16828 (2023).

[2] S. Grimme, Semiempirical gga-type density functional constructed with a long-range dispersion correction, Journal of computational chemistry **27**, 1787 (2006).
[3] S. Grimme, S. Ehrlich, and L. Goerigk, Effect of the damping function in dispersion corrected density functional theory, Journal of computational chemistry **32**, 1456 (2011).
[4] E. M. Lifshitz, L. Pitaevskii, and V. Berestetskii, Landau and lifshitz course of theoretical physics, Statistical physics **5** (1980).
[5] P. C. Hohenberg and A. P. Krekhov, An introduction to the ginzburg–landau theory of phase transitions and nonequilibrium patterns, Physics Reports **572**, 1 (2015).